LBNL-39869
UC-1240

Application of Inverse Modeling to Geothermal Reservoir Simulation

S. Finsterle[1], K. Pruess[1], D.P. Bullivant[2], and M.J. O'Sullivan[2]

[1] Earth Sciences Division
Lawrence Berkeley National Laboratory
University of California
Berkeley, CA 94720

[2] Department of Engineering Science
University of Auckland
Auckland, New Zealand

Paper presented at the
Twenty-Second Workshop on Geothermal Reservoir Engineering
Stanford University, Stanford, California
January 27-29, 1997,
and to be published in the Proceedings

January 1997

This work was supported, in part, by the Assistant Secretary for Energy Efficiency and Renewable Energy, Office of Geothermal Technologies, of the U.S. Department of Energy under contract No. DE-AC03-76SF00098.

PROCEEDINGS, Twenty-Second Workshop on Geothermal Reservoir Engineering
Stanford University, Stanford, California, January 27-29, 1997
SGP-TR-155

APPLICATION OF INVERSE MODELING TO GEOTHERMAL RESERVOIR SIMULATION

S. Finsterle[1], K. Pruess[1], D.P. Bullivant[2], and M.J. O'Sullivan[2]

[1] Lawrence Berkeley National Laboratory, Earth Sciences Division, Berkeley, CA 94720
[2] Department of Engineering Science, University of Auckland, Auckland, New Zealand

ABSTRACT

We have developed inverse modeling capabilities for the non-isothermal, multiphase, multicomponent numerical simulator TOUGH2 to facilitate automatic history matching and parameter estimation based on data obtained during testing and exploitation of geothermal fields. The ITOUGH2 code allows one to estimate TOUGH2 input parameters based on any type of observation for which a corresponding simulation output can be calculated. Furthermore, a detailed residual and error analysis is performed, and the uncertainty of model predictions can be evaluated. Automatic history matching using ITOUGH2 is robust and efficient so that model parameters affecting geothermal field performance can reliably be estimated based on a variety of field measurements such as pressures, temperatures, flow rates, and enthalpies. The paper describes the methodology of inverse modeling and provides a detailed discussion of sample problems to demonstrate the application of the method to data from geothermal reservoirs.

INTRODUCTION

Development of a numerical model for predicting the performance of a geothermal field requires several steps. First, the complex physical processes controlling multiphase fluid flow and heat transport in fractured-porous media have to be described. Furthermore, a site-specific model has to be built, i.e., the geometry of the reservoir, its hydrogeological and thermophysical properties, as well as initial and boundary conditions have to be determined. After parameter values have been assigned, predictive reservoir simulation can be initiated. Parameter values can be obtained from laboratory measurements or by calibrating the model against data collected during well testing or field exploitation. It is important to realize that the estimated parameters are both conceptually and numerically related to the structure of the model. The fact that parameters estimated by inverse modeling may not necessarily represent an intrinsic property of a reservoir but actually depend on the model being used is often considered a drawback. However, the problem occurs regardless of the method being used to determine parameter values, including direct measurements of rock properties on core samples. By definition, inverse modeling provides the parameter set best suited to reproduce the observed reservoir behavior. It can therefore be considered adequate to produce reliable predictions provided that the simulations are based on a consistent conceptual model of the geothermal reservoir.

In this paper we discuss the determination of model-related reservoir parameters by automatically calibrating a numerical model against data obtained during well testing or exploitation of a geothermal field. We first describe the modeling approach used to simulate fluid and heat flow in fractured-porous media. The inverse problem is then formulated in the framework of maximum likelihood theory, followed by a brief discussion of the optimization algorithm. A sample problem is given to demonstrate the application of the method to (synthetic) field performance data, and preliminary results are shown from an effort to calibrate actual field data.

MODELING APPROACH

Fluid and heat flow in a geothermal field is simulated using the TOUGH2 code (Pruess, 1991). Solving the forward problem in an efficient and stable manner is the most important step for automatic parameter estimation. TOUGH2 is used here to simulate non-isothermal flow of a single component (water) in two coexisting phases (liquid, vapor). The mass and energy balance equations for an arbitrary subdomain V_n bounded by the surface Γ_n can be written in the following form:

$$\frac{\mathrm{d}}{\mathrm{d}t}\int_{V_n} M \,\mathrm{d}V = \int_{\Gamma_n} \mathbf{F}\bullet\mathbf{n}\,\mathrm{d}\Gamma + \int_{V_n} q\,\mathrm{d}V \tag{1}$$

The accumulation term M represents mass (m) or internal energy (h) per unit reservoir volume:

$$M_m = \phi\,(S_l\,\rho_l + S_v\,\rho_v) \tag{2}$$

$$M_h = \phi\,(S_l\,\rho_l\,u_l + S_v\,\rho_v\,u_v) + (1 - \phi)\,\rho_R\,C_R\,T \tag{3}$$

Here ϕ is porosity, S is saturation, ρ is density, u is internal energy, C is specific heat, and T is temperature. The subscripts l, v, and R denote liquid, vapor, and rock, respectively. The mass flux is a sum over the fluxes in the liquid and vapor phase:

$$\mathbf{F}^{m} = \sum_{\beta=l,v} -\mathbf{k}\frac{k_{r\beta}}{\mu_{\beta}}\rho_{\beta}\left(\nabla P_{\beta} - \rho_{\beta}\,\mathbf{g}\right) \qquad (4)$$

where $\mathbf{k}$ denotes the permeability tensor, k_r is relative permeability, μ is viscosity, P_β is the pressure in phase β, and $\mathbf{g}$ is acceleration of gravity. In Eq. 1, $\mathbf{n}$ is the inward unit normal vector. The total heat flux containing conductive and convective components can be written as follows:

$$\mathbf{F}^{h} = -K\nabla T + \sum_{\beta=l,v}\left(h_{\beta}\,\mathbf{F}_{\beta}\right) \qquad (5)$$

with K the thermal conductivity of the rock-fluid mixture, h_β the specific enthalpy, which is a non-linear function of temperature, and $\mathbf{F}_\beta$ the mass flux in phase β (see Eq. 4). Thermophysical properties of liquid water and vapor are calculated using steam table equations given by the International Formulation Committee (IFC, 1967). The continuum equations (1) are discretized in space based on an integral finite difference formulation (Narasimhan and Witherspoon, 1976), and a multiple interacting continua (MINC; Pruess and Narasimhan, 1985) approach is used to represent fractured-porous media. Time is discretized fully implicitly as a first-order finite difference. Discretization results in a set of nonlinear coupled algebraic equations which are solved simultaneously by means of Newton-Raphson iterations. A conjugate gradient method is used to solve the linear equations arising at each iteration.

THE INVERSE PROBLEM

The determination of reservoir properties from performance data, such as pressures, temperatures, and flow rates, is referred to as the inverse problem. The indirect approach to inverse modeling consists of minimizing the differences between the observed and simulated field responses, which are assembled in the residual vector $\mathbf{r}$ with elements

$$r_i = y_i^* - y_i(\mathbf{p}) \qquad (6)$$

Here y_i^* is an observation (e.g., pressure, temperature, flow rate, etc.) at a given point in space and time, and y_i is the corresponding simulator prediction, which depends on the vector $\mathbf{p}$ of all unknown or uncertain model parameters, including initial and boundary conditions. If the error structure of the residuals is assumed Gaussian and described by a covariance matrix $\mathbf{C}$, the objective function to be minimized is simply the sum of the squared residuals weighted by the inverse of the prior covariance matrix:

$$z(\mathbf{p}) = \mathbf{r}^{T}\,\mathbf{C}^{-1}\,\mathbf{r} \qquad (7)$$

In maximum likelihood theory, it can be shown that minimizing z is equivalent to maximizing the probability of reproducing the observed system state. Eq. 7 corresponds to the generalized nonlinear least squares estimator.

Due to the strong nonlinearities of function $y_i(\mathbf{p})$, an iterative procedure is required to minimize the objective function. The Levenberg-Marquardt modification of the Gauss-Newton algorithm (Levenberg, 1944; Marquardt, 1963) has been found to be the most robust for our purposes. The basic idea of this method is to move in the parameter space along the steepest descent direction far from the minimum, switching continuously to the Gauss-Newton algorithm as the minimum is approached. This is achieved by decreasing a scalar λ, known as the Levenberg parameter, after a successful iteration, but increasing it if an uphill step is taken. The following system of equations is solved for $\Delta\mathbf{p}$ at an iteration labeled k:

$$(\mathbf{J}_k^{T}\,\mathbf{C}^{-1}\,\mathbf{J}_k + \lambda_k\mathbf{D}_k)\,\Delta\mathbf{p}_k = -\mathbf{J}_k^{T}\,\mathbf{C}^{-1}\,\mathbf{r}_k \qquad (8)$$

Here, $\mathbf{J}$ is the sensitivity matrix with elements $J_{ij} = -\partial r_i/\partial p_j = \partial y_i/\partial p_j$. $\mathbf{D}$ denotes a matrix of order n (n being the number of parameters to be estimated) with elements equivalent to the diagonal elements of matrix $(\mathbf{J}_k^{T}\,\mathbf{C}^{-1}\,\mathbf{J}_k)$. The improved parameter set is finally calculated:

$$\mathbf{p}_{k+1} = \mathbf{p}_k + \Delta\mathbf{p}_k \qquad (9)$$

Under the assumption of normality and linearity, a detailed error analysis of the final residuals and the estimated parameters can be conducted (for details see Finsterle and Pruess (1995)). For example, the covariance matrix of the estimated parameter set is given by:

$$\mathbf{C}_{pp} = \frac{\mathbf{r}^{T}\,\mathbf{C}^{-1}\,\mathbf{r}}{m-n}\,(\mathbf{J}^{T}\,\mathbf{C}^{-1}\,\mathbf{J})^{-1} \qquad (10)$$

where m is the total number of observations. As a byproduct of calculating the Jacobian matrix $\mathbf{J}$, one can qualitatively examine the contribution of each data point to the solution of the inverse problem as well as the total parameter sensitivity.

The inverse modeling formulation outlined above is implemented in a computer program named ITOUGH2 (Finsterle, 1993).

SYNTHETIC EXAMPLE

The purpose of this section is to illustrate the use of the proposed methodology for the characterization of geothermal reservoirs. ITOUGH2 provides the flexibility to take advantage of any type of data usually collected during field exploitation. For the sake of simplicity and reproducibility, we will analyze a synthetic case. A preliminary application of ITOUGH2 to actual data is discussed in the next section.

We consider a two-dimensional five-spot production-injection problem (see Fig. 1) previously studied by Pruess (1991) and Pruess and Wu (1993). The problem specifications correspond to conditions typically encountered in deeper zones of two-phase geothermal reservoirs. The medium is assumed to be fractured with embedded impermeable matrix blocks in the shape of cubes with side lengths of 50 m. The permeable volume fraction is 2 % with a porosity of the fracture domain of 50 %. Reservoir thickness is 305 m. Water with an enthalpy of 500 kJ/kg is injected at a rate of 30 kg/s. Production rate is also 30 kg/s.

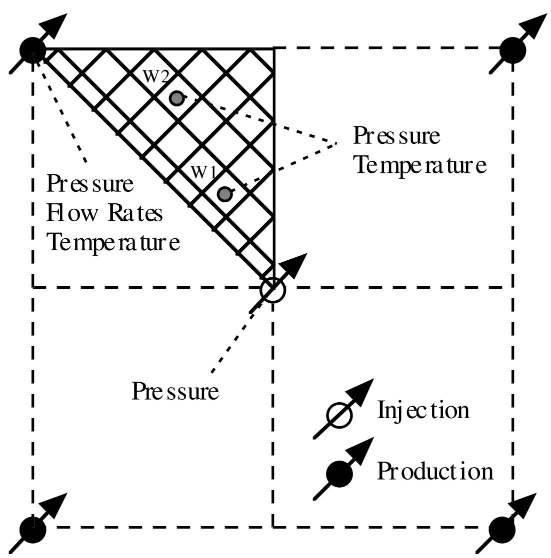

Fig. 1. Five-spot well pattern with grid for modeling 1/8 symmetric domain. Observation points and type of data measured is also indicated.

We assume that temperature and pressure measurements are taken in the injection (Inj) and production well (Pro) as well as in two abandoned wells (W1, W2; see Fig. 1). Furthermore, liquid and vapor flow rates are measured in the production well. Note that temperature and pressure measurements are redundant as long as two-phase conditions prevail. TOUGH2 is run in forward mode to generate synthetic data for five years of field performance history, and random noise is added to simulate measurement errors (see Table 1 for standard deviations).

Subsequently, the model is automatically calibrated against these observations in order to determine certain input parameters considered unknown or uncertain. The parameters include the effective permeability of the fracture system, porosity, heat conductivity, specific heat of the rock grains, fracture spacing a (which is a parameter of the MINC preprocessor), and the initial reservoir temperature T_i.

The estimated parameter set is shown in Table 2. The covariance and correlation matrices are summarized in Table 3, and some statistical measures are given in Table 4. The latter need some explanations. The second column of Table 4 contains the standard deviation σ_p of the estimate which is the square root of the corresponding diagonal element in Table 3.

Table 1. Observations Used for Model Calibration

Data Type	Location	Standard Dev.
Pressure	Inj/Pro/W1/W2	2.00 bar
Temperature	Pro/W1/W2	5.00 ˚C
Liquid flow rate	Pro	1.60 kg/s (~5 %)
Vapor flow rate	Pro	0.08 kg/s (~5 %)

Table 2. True, Initial, and Estimated Parameter Set

Parameter	True Value	Initial Guess	Best Estimate
log (perm. [m^2])	-14.22	-13.00	-14.22
fracture porosity [-]	0.50	0.30	0.56
specific heat [J/kg˚C]	1000.00	800.00	971.00
heat cond. [W/m˚C]	2.10	2.50	2.25
fracture spacing [m]	50.00	20.00	50.50
temperature [˚C]	300.00	250.00	300.10

Table 3. Variance-Covariance Matrix (Main Diagonal and Lower Triangle) and Correlation Matrix (Upper Triangle)

	log(k)	ϕ	C_R	K	a	T_i
log(k)	5E-6	0.21	0.17	-0.25	-0.21	-0.18
ϕ	2E-5	2E-3	0.17	-0.23	-0.18	-0.04
C_R	0.01	0.23	845	0.39	0.53	-0.07
K	-5E-4	-0.01	10.15	0.79	0.98	0.29
a	-4E-3	-0.08	14.52	8.27	89.22	0.19
T_i	-4E-5	-2E-4	0.24	0.02	0.20	0.01

Table 4. Statistical Measures and Parameter Sensitivity

Parameter	Standard Deviation	$\sigma_p{}^*/\sigma_p$	Parameter Sens.
log (perm. [m^2])	0.002	0.88	3623.1
fracture porosity [-]	0.05	0.90	19.6
specific heat [J/kg˚C]	29.10	0.03	64.7
heat cond. [W/m˚C]	0.89	0.18	50.5
fracture spacing [m]	9.40	0.03	253.6
temperature [˚C]	0.10	0.94	1768.2

Note that the standard deviation shown in Table 4 refers to the joint probability density function, i.e., it takes into account the uncertainty of the parameter itself and the influence from correlated parameters. The conditional standard deviation $\sigma_p{}^*$, on the other hand, reflects the uncertainty of an estimate provided that all the other parameters are exactly known. Therefore, the ratio $\sigma_p{}^*/\sigma_p$ shown in the third column of Table 4 is a measure of how independently a parameter can be estimated. A value close to one indicates an independent estimate, whereas small values can be interpreted as a loss of parameter identifiability due to its correlation to other uncertain parameters. Finally, we show the total parameter sensitivity (column 4) which is the sum of the absolute values of all sensitivity coefficients, weighted by the inverse of individual measurement errors and scaled by a reasonable parameter variation.

First we note that permeability and reservoir temperature are accurately identified. They are the most sensitive parameters and can be determined almost independently. The estimates of fracture spacing, heat conductivity and specific heat exhibit relatively high standard deviations which is easily explained by the large correlation coefficients among these three parameters (see Table 3). Especially the fracture spacing and heat conductivity have a high positive correlation coefficient, i.e., a larger fracture spacing can be almost completely compensated by an increase in heat conductivity. This statement is true for the type and amount of data available, i.e., the correlation between these two parameters may be reduced by taking additional data. Finally, the fracture porosity can be relatively well determined despite its low overall sensitivity. This is simply due to the fact that fracture porosity is only weakly correlated to the other parameters, resulting in an independent estimate.

The system response as observed in the injection, production and observation wells is shown in Fig. 2. The squares are the synthetically generated and perturbed data points used to calibrate the model. The triangles represent the future system response for the true parameter set (see Table 2, column 2). The solid lines are the pressures, temperatures, water and vapor flow rates simulated using the estimated parameter set (Table 2). For the first 5 years, the deviations between the solid lines and the squares minimize Eq. 7. Beyond 5 years, the solid lines are predictions, i.e., an extrapolation of the system response matched during the calibration period. The model predictions are uncertain due to uncertainties in the estimated parameters. The standard deviation of the calculated system response, i.e., the uncertainty of the predicted temperature in the production well at a certain point in time, is the square root of the corresponding diagonal element of matrix $\mathbf{C}_{zz}$ which is calculated using first-order error propagation analysis:

$$\mathbf{C}_{zz} = \mathbf{J}\,\mathbf{C}_{pp}\,\mathbf{J}^T \qquad (11)$$

Here, matrix $\mathbf{J}$ is the sensitivity matrix for the predicted system response, and $\mathbf{C}_{pp}$ is the covariance matrix of the estimated parameters (Eq. 10). The resulting 95% error bands on the model predictions are shown as dash-dotted lines in Fig. 2. They have to be considered optimistic because only the uncertainty of the six selected parameters is taken into account. All the other parameters as well as the model structure are assumed to be exactly known, which is only true for a synthetic case. However, it is interesting to note that the true system response (triangles) lies within the estimated error band despite the fact that the parameter set used for the prediction does not exactly correspond to the true one (Table 2).

The high accuracy of the model prediction can only be achieved by a combined inversion of all available data. It is obvious that the temperature decrease in observation well W1 could not have been predicted by relying only on temperature data during the calibration phase. In fact, the contribution of temperature measurements to the determination of the parameter set is minor. This is mainly due to the fact that a temperature change of 1 °C leads to a vapor pressure change of about 1 bar which can be more easily detected given the assumed accuracy of pressure measurements.

Table 5. Total Sensitivity of Observations, Standard Deviation of Residuals, and Contribution to Objective Function.

Observation	Sensitivity	Std. Dev.	COF
Pressure Inj.	789	1.9	9.7
Pressure Pro.	1500	2.0	10.3
Pressure W1	426	2.2	12.5
Pressure W2	358	2.1	11.6
Temp. Pro.	680	4.6	8.9
Temp. W1	107	5.4	12.2
Temp. W2	100	5.2	11.3
Water flow rate	87	1.6	10.5
Vapor flow rate	1735	0.1	13.0

COF: Contribution to Objective Function [%]

Provided that the expected measurement errors (see Table 1, column 3) are reasonable, the bulk of the information about the parameters of interest is contained in the accurate vapor flow rate measurements and the pressure data in the production well. The contribution of a certain observation (e.g., flow rate data of a given accuracy taken over the entire measurement period) to the solution of the inverse problem can be evaluated by adding all the absolute values of the corresponding sensitivity coefficients, weighted by the expected measurement error and scaled by the inverse of the parameter variation. This qualitative measure is summarized in Table 5, column 2. Comparing total sensitivities of individual observations, one can conclude that accurate measurements of vapor flow rates and pressures and temperatures in the injection and production wells would be sufficient to solve the inverse problem, i.e., data from the observation wells are less sensitive in our example.This kind of an analysis can be performed without actually collecting data, i.e., it can be used to design and optimize monitoring systems. Details of such a procedure are described in Finsterle and Pruess (1996).

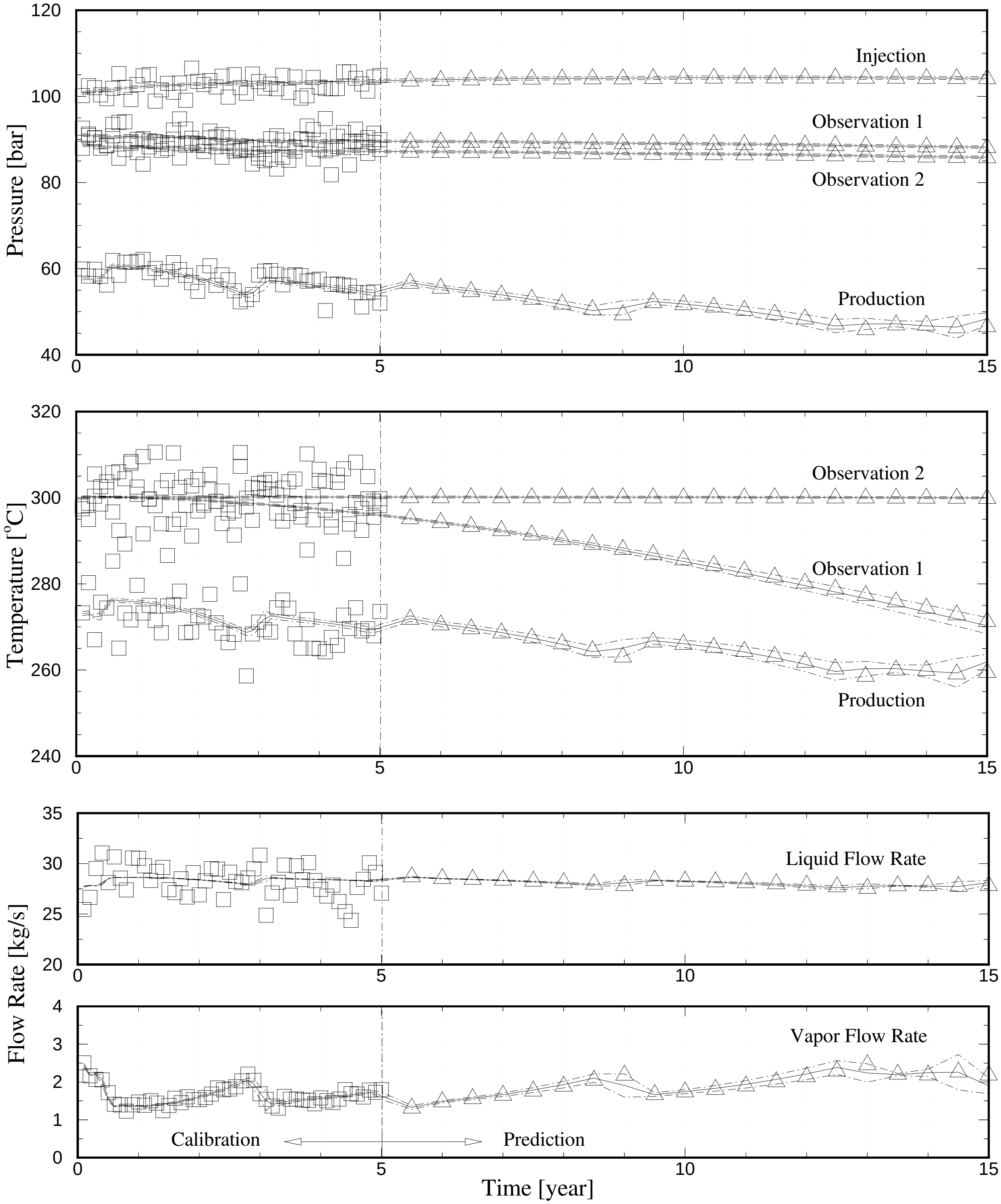

Fig. 2. Synthetic example: Calibration and prediction of pressures, temperatures, water and vapor flow rates. Squares are synthetic data points used for calibration. Triangles represent the true system response. Simulation results based on the estimated parameter set are shown as solid lines. Error bands (dash-dotted lines) are calculated using linear error propagation analysis.

The standard deviations of the final residual (Table 5, column 3) are on the order of the measurement errors, indicating that no significant systematic errors are present. Finally, the contribution of each observation type to the final value of the objective function (Table 5, column 4) is evenly distributed among the measurements, rendering the choice of the weighting factors in matrix $\mathbf{C}^{-1}$ reasonable.

Recall that this study uses synthetic data with known error structure, and that no systematic errors are made because the conceptual model is correct. In field applications, the proper conceptual model and the structure of the random errors are not exactly known. Note, however, that the relative weighting of data points can easily be adjusted and is partly automated in ITOUGH2 following the suggestions by Carrera and Neuman (1986).

While the problem of systematic errors is not directly addressed by inverse modeling, the automation of the calibration step makes it possible to examine a number of alternative conceptual models. The extensive residual analysis performed by ITOUGH2 provides a means to identify aspects of the model that need to be refined. Moreover, model identification criteria (Carrera and Neuman, 1986) are evaluated which help select the model that most likely represents field conditions.

APPLICATION

ITOUGH2 has been successfully applied to a variety of problems involving laboratory and field data (see e.g., Finsterle and Persoff, 1996; Finsterle and Pruess, 1995; 1996). Applications of ITOUGH2 to geothermal field data are described in O'Sullivan and Bullivant (1995), and White (1995).

In this section we present preliminary results of an inversion of pressure and enthalpy data from a geothermal well, using a simple, one-dimensional, radial model with homogeneous rock properties. The thickness of the reservoir is assumed to be 200 m; the feed zone is at a depth of about 1600 m. Initial reservoir temperature was measured to be 336 ˚C.

Note that the pressure and enthalpy data were obtained at the wellhead whereas the simulation results refer to downhole conditions. While heat loss and enthalpy changes along the wellbore are not expected to be large, the pressure drop is significant and a function of flow rates and phase composition. A wellbore simulator would have to be connected to the reservoir simulator to accurately model wellhead pressures. In this preliminary study, we assume the pressure drop to be independent of flow rate, and it will be treated as an unknown parameter to be simultaneously estimated with the reservoir properties.

The parameters to be estimated are selected based on a sensitivity analysis. Only the most sensitive parameters of relative low overall correlation are subjected to the estimation process. They include the logarithm of the absolute permeability, porosity, initial vapor saturation, residual liquid saturation, the van Genuchten parameter n in the relative permeability function (Luckner et al., 1989), and a constant c_{well} representing the pressure drop along the wellbore.

Data from 85 days of production were used to calibrate the model. The production rate during this period varied around 4 kg/s. Data are again available after t=106 days, where production rate was increased to about 10 kg/s. This latter period was not used for calibration, but for testing the model predictions. Fig. 3 shows the prescribed production rate, the observed and calculated enthalpies and pressures for the initial parameter set as well as the best estimate, along with the 95 % error band. The corresponding parameter sets are given in Table 6.

Comparison of the responses obtained with the initial and final parameter set demonstrates the sensitivity of the modeling results with respect to the relatively minor updates needed to improve the match. More important, it reveals the difficulties of the current model to simulate the relatively strong pressure drop between t=55 and t=70, without yielding too low pressures once the production rate is increased. Recall that wellbore effects are not modeled. While the enthalpies are matched reasonably well except at early times, where fracture flow may be dominant, the model fails to predict the enthalpy during the last period of high production, where most of the produced fluid in the model consists of vapor.

It should be realized that the conditions during the validation phase are quite different from the ones encountered while calibrating the model. Vapor saturation near the well is increased, i.e., the relative permeabilities are extrapolated beyond the calibrated range. We mention in passing that the van Genuchten model performs best compared to a number of competing models. It is obvious that systematic errors have to be eliminated before the parameter set can be further assessed.

Table 6. Initial, Best Estimate, and Uncertainty

Parameter	Initial Guess	Best Estimate	Standard Deviation
log (perm. [m^2])	-14.50	-14.48	0.01
porosity [-]	0.02	0.05	0.01
initial vapor sat. [-]	0.02	0.01	0.01
res. liq. sat. [-]	0.20	0.18	0.04
vG parameter n [-]	3.00	2.45	0.08
c_{well} [bar]	40.00	45.40	1.14

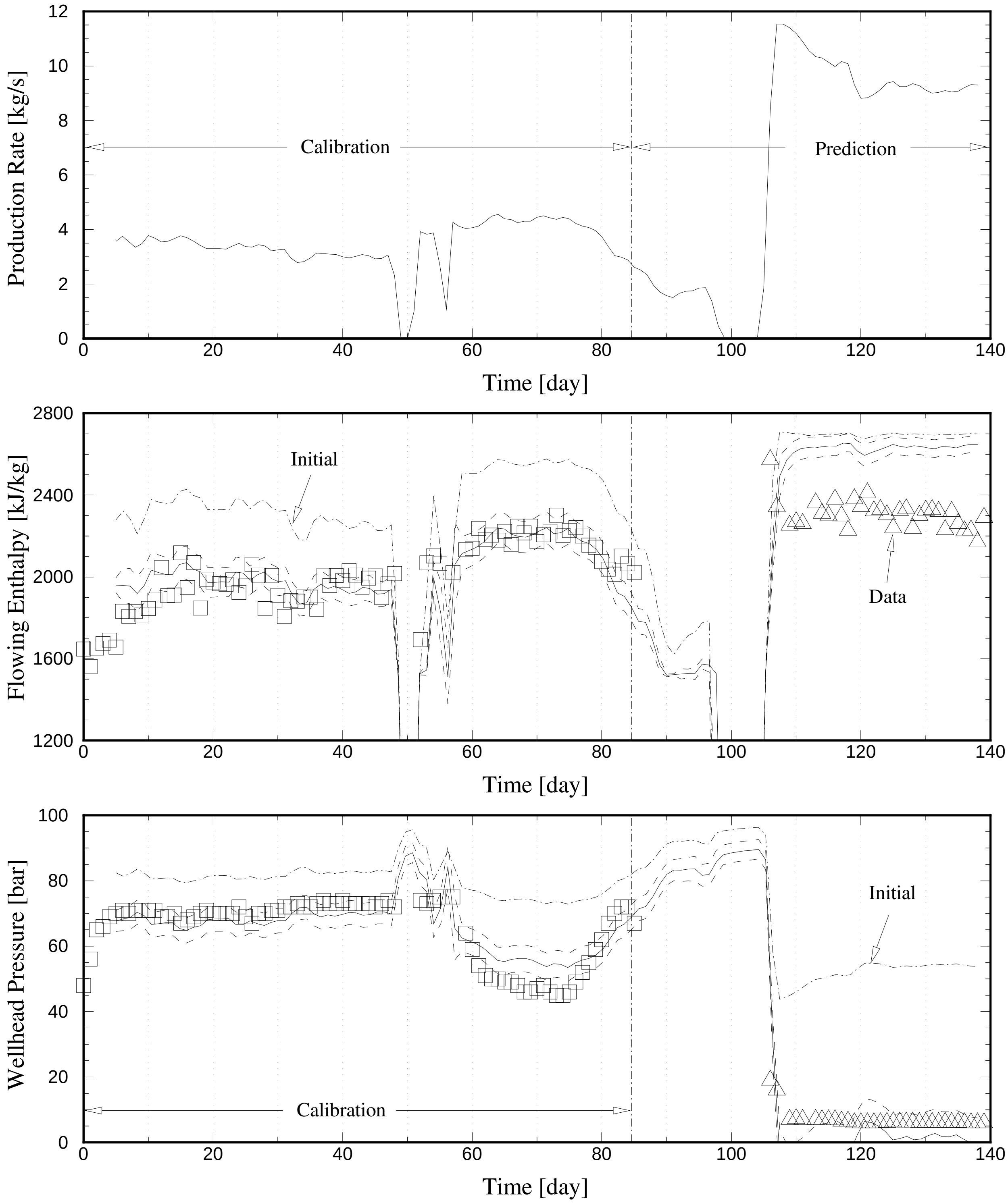

Fig. 3. Application case: Calibration and prediction of flowing enthalpy and wellhead pressure. The top panel shows the prescribed production rate. Squares are measured data used for calibration. Triangles are measured data used for validation. The dash-dotted lines are the model results with the initial parameter set (see Table 6). Simulation results based on the estimated parameter set are shown as solid lines. Error bands (dashed lines) are calculated using linear error propagation analysis.

CONCLUDING REMARKS

The purpose of this study was to demonstrate the flexibility of an inverse modeling approach for automatic history matching and the estimation of model parameters by performing a joint inversion of all available data. In addition to automatic model calibration, the ITOUGH2 code provides a number of semi-quantitative measures to study parameter sensitivities, correlations between parameters and observations, prediction uncertainties, total parameter sensitivities, and the potential benefit from taking measurements of a certain kind and in a certain location. This information is useful for the design and optimization of reservoir delineation and monitoring programs.

The advantage of inverse modeling procedures is that they overcome the time and labor-intensive tedium of trial-and-error model calibration. Effective, model-related parameters are automatically determined on the scale of interest. This ensures that the reliability of subsequent predictions can be improved if they are based on the same or a consistent conceptual model of the geothermal reservoir.

In order to take full advantage of inverse modeling, it is imperative to minimize systematic errors in the conceptual model. We plan to incorporate a flowing wellbore pressure correction into ITOUGH2 to eliminate the bias introduced when using pressure data for calibration.

ACKNOWLEDGMENT

This work was supported, in part, by the Assistant Secretary for Energy Efficiency and Renewable Energy, Office of Geothermal Technologies, of the U.S. Department of Energy under Contract No. DE-AC03-76SF00098. We would like to thank E. Sonnenthal and M. Lippmann for thoughtful reviews.

REFERENCES

Carrera, J. and S.P. Neuman (1986), "Estimation of Aquifer Parameters Under Transient and Steady State Conditions: 1. Maximum Likelihood Method Incorporating Prior Information," *Water Resour. Res.*, *22*(2), 199-210.

Finsterle, S. (1993), "ITOUGH2 User's Guide, Version 2.2," Report LBNL-34581, Lawrence Berkeley National Laboratory, Berkeley, Calif.

Finsterle, S. and K. Pruess (1995), "Solving the Estimation-Identification Problem in Two-Phase Flow Modeling," *Water Resour. Res.*, *31*(4), 913-924.

Finsterle, S. and K. Pruess (1996), "Design and Analysis of a Welltest for Determining Two-Phase Hydraulic Properties," Report LBL-39620, Lawrence Berkeley National Laboratory, Berkeley, Calif.

Finsterle, S., and P. Persoff (1996), "Determining Permeability of Tight Rock Samples Using Inverse Modeling," Report LBL-39296, Lawrence Berkeley National Laboratory, Berkeley, Calif.

International Formulation Committee (1967), "A Formulation of the Thermodynamic Properties of Ordinary Water Substance," IFC Secretariat, Düsseldorf, Germany.

Levenberg, K. (1944), "A Method for the Solution of Certain Nonlinear Problems in Least Squares," *Q. Appl. Math.*, 2, 164-168.

Luckner, L., M. T. van Genuchten, and D. Nielsen (1989), "A Consistent Set of Parametric Models for the Two-Phase Flow of Immiscible Fluids in the Subsurface, *Water Resour. Res.*, *25*(10), 2187-2193.

Marquardt, D.W. (1963), "An Algorithm for Least-Squares Estimation of Nonlinear Parameters," *J. Soc. Ind. Appl. Math.*, *11*(2), 431-441.

Narasimhan, T.N. and P.A. Witherspoon (1976), "An Integrated Finite Difference Method for Analyzing Fluid Flow in Porous Media," *Water Resour. Res.*, *12*(1), 57-64.

O'Sullivan, M.J. and D.P. Bullivant (1995), "Inverse Modelling of the Wairakei Geothermal Field Using ITOUGH2," *paper presented at the 17th New Zealand Geothermal Workshop*, Auckland, New Zealand.

Pruess, K. and T.N. Narasimhan (1985), "A Practical Method for Modeling Fluid and Heat Flow in Fractured Porous Media," *Soc. Pet. Eng. J.*, *25*(1), 14-26.

Pruess, K. (1991), "TOUGH2 - A General-Purpose Numerical Simulator for Multiphase Fluid and Heat Flow," Report LBL-29400, Lawrence Berkeley National Laboratory, Berkeley, Calif.

Pruess, K. and Y.-S. Wu (1993), "A New Semi-Analytical Method for Numerical Simulation of Fluid and Heat Flow in Fractured Reservoirs," *SPE Advanced Technology Series*, Vol. 1, No. 2, 63-72, Richardson, Texas.

White, S.P. (1995), "Inverse Modelling of the Kawerau Geothermal Reservoir, NZ," *Proceedings,* 17th New Zealand Geothermal Workshop, Auckland, New Zealand, 211-216.